Moisture variations in a developing cyclone as measured by airborne GPS remote sensing

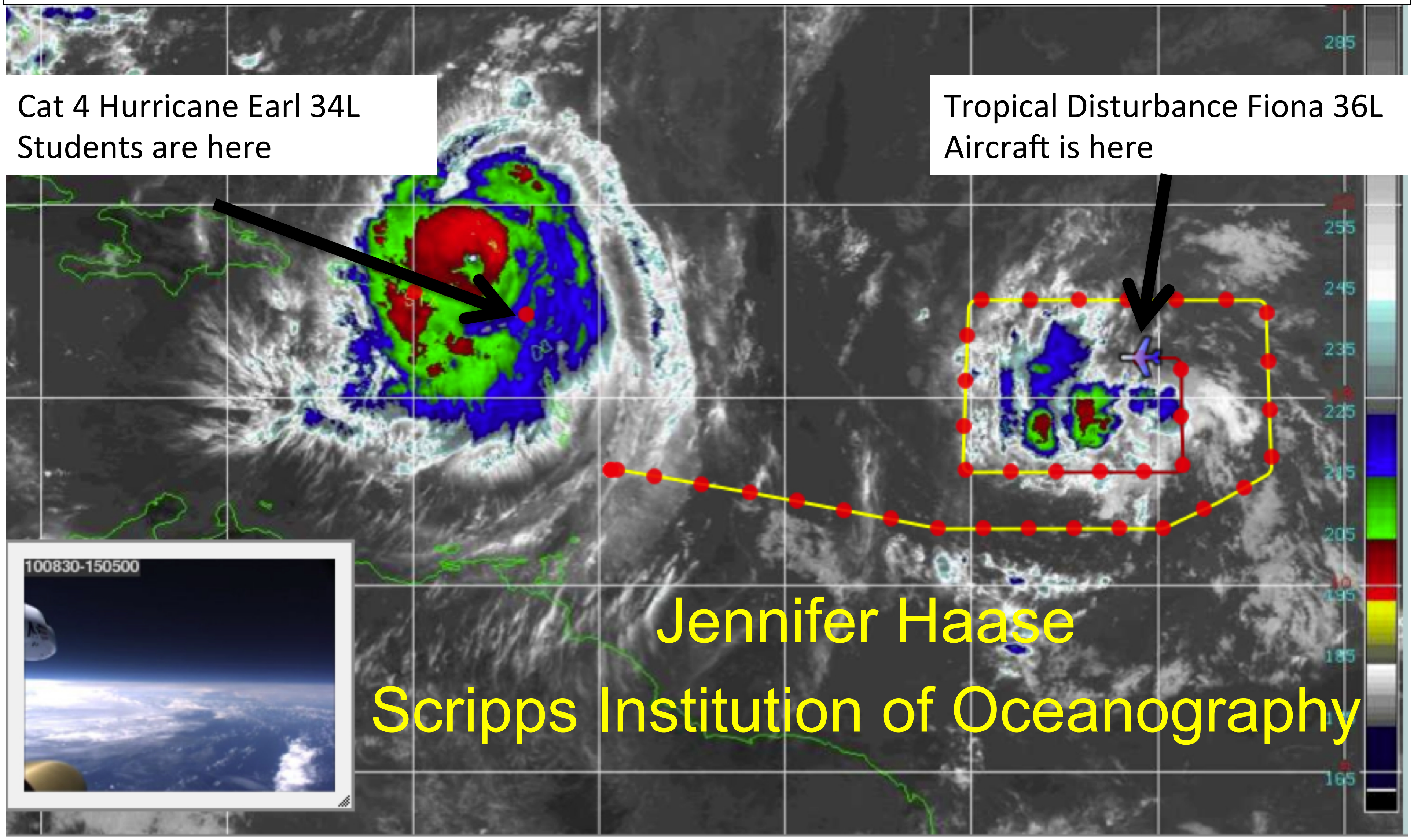

Jennifer Haase
Scripps Institution of Oceanography

Acknowledgements

- Brian Murphy, Paytsar Muradyan, Alexandria Johnson
  - Purdue Earth and Atmospheric Sciences
- James Garrison, Ulvi Acikoz, Eric Wang
  - Purdue Aeronautical and Astronautical Engineering
- Shu-Hua Chen, Xue Meng Chen
  - UC Davis
- Michael Montgomery
  - Naval Postgraduate School
- Chris Davis
  - National Center for Atmospheric Research
- *Sponsored by NSF AGS – 1015904*

Overview

- Description of the airborne GPS remote sensing system
- PRE-Depression Investigation of Cloud systems in the Tropics
- Measuring moisture evolution during hurricane development

Airborne GPS radio occultation

- Side-looking GPS receiver tracks setting and rising satellites
- Nearly horizontal raypaths experience refractive delay
- Atmospheric humidity profile is derived from refractive delay

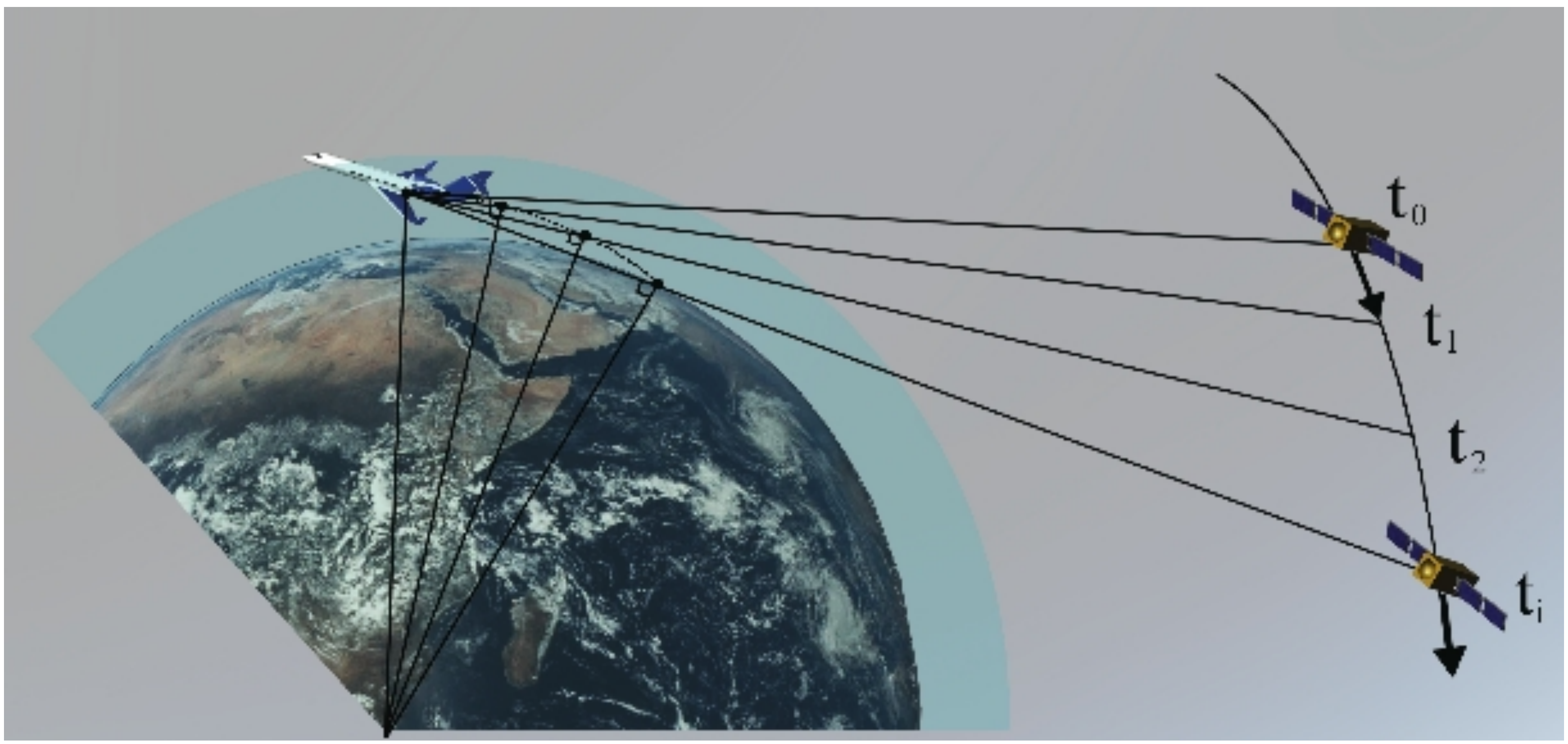

Refractive bending angle

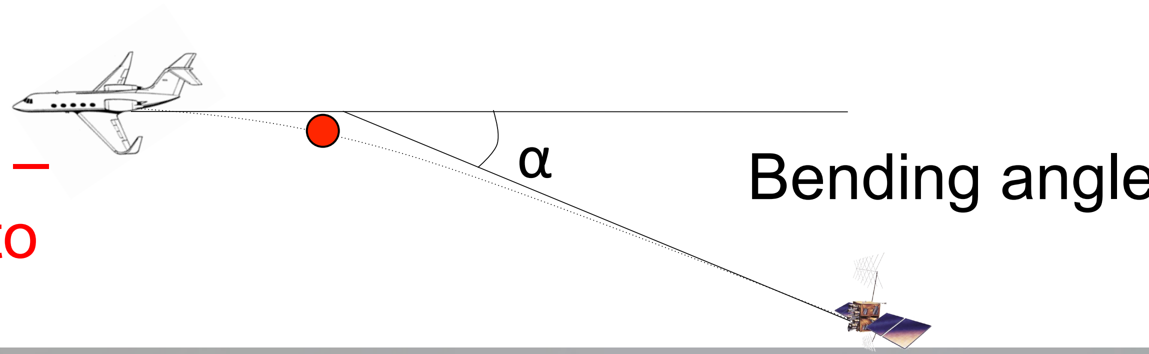

Tangent point – point closest to Earth surface

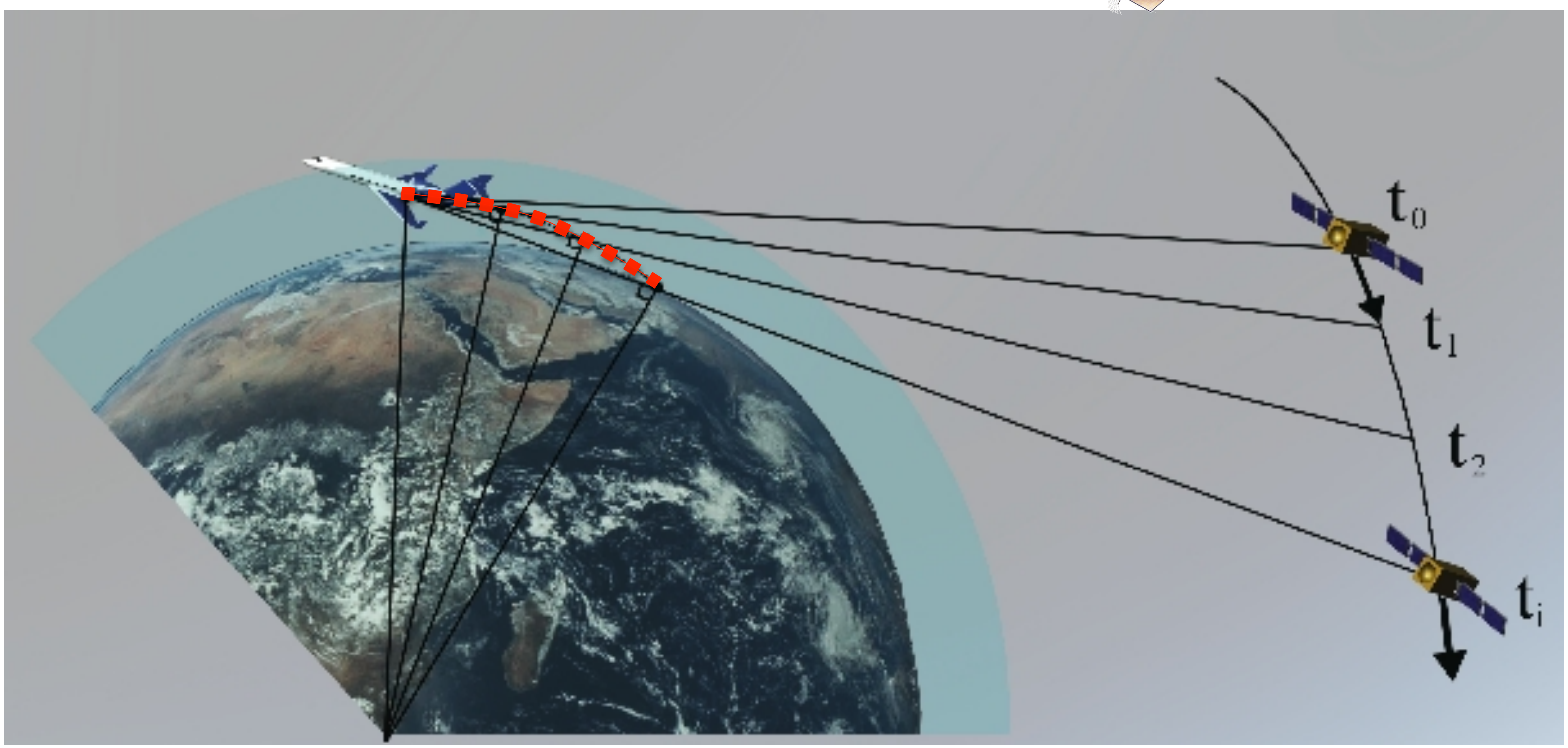

GPS refractive delay

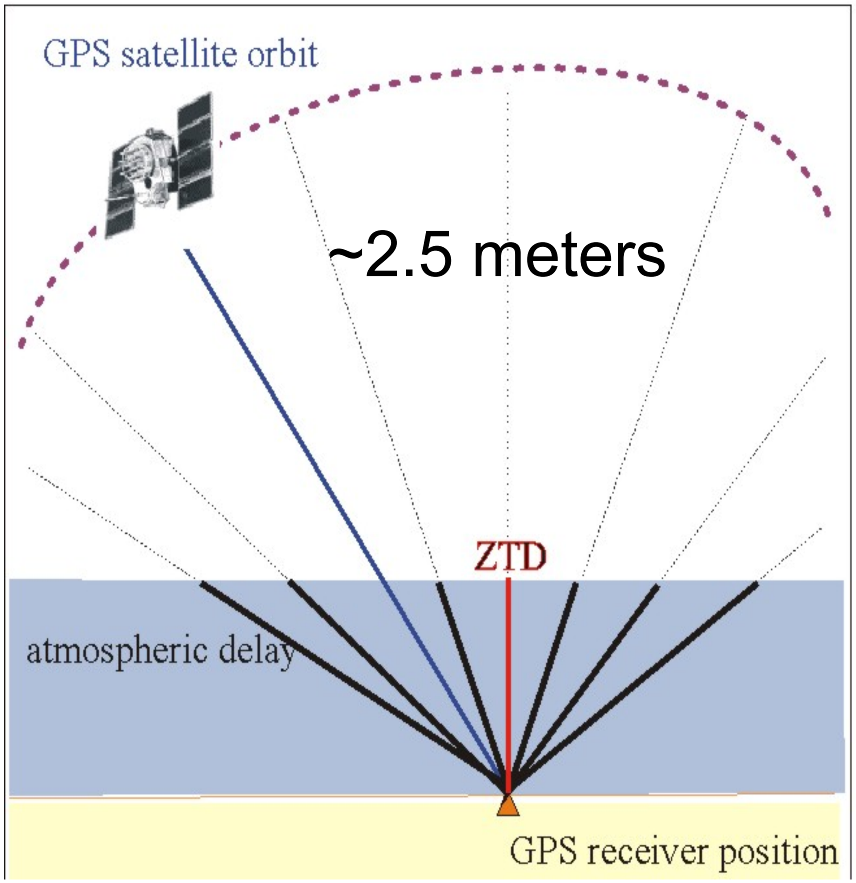

$$ZTD = \int_z N(z) \cdot 10^{-6}\, dz$$

$$N = k_1 \frac{P_d}{T} + k_2 \frac{e}{T} + k_3 \frac{e}{T^2}$$

$$excess\ phase(m) = L1m - geom.dist - sat.clk\ error - rel.eccent.corr. - iono.corr.$$

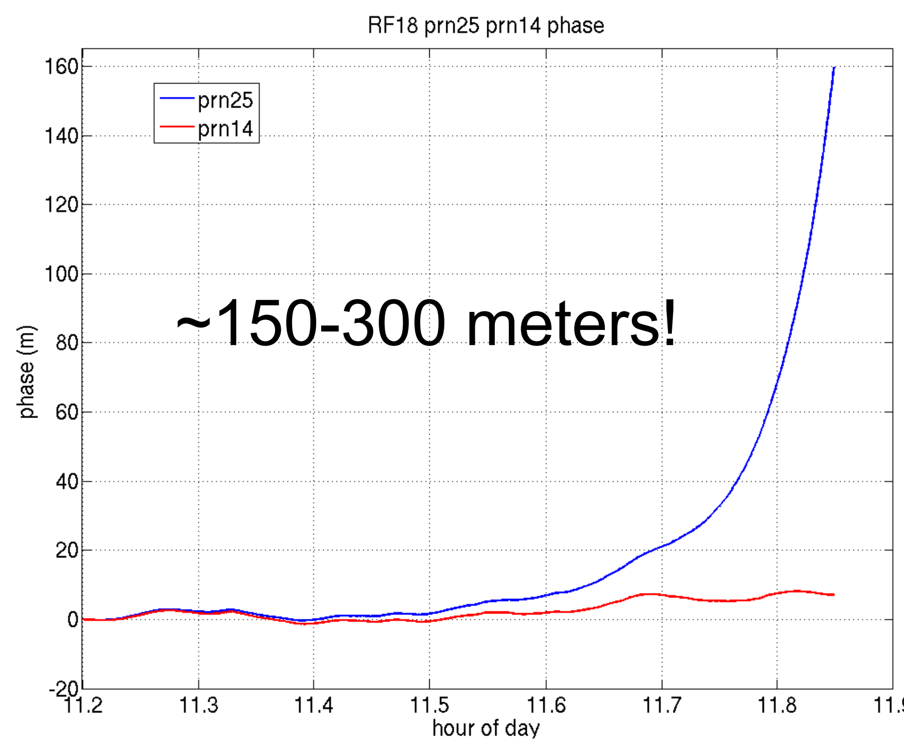

GISMOS installed on research aircraft

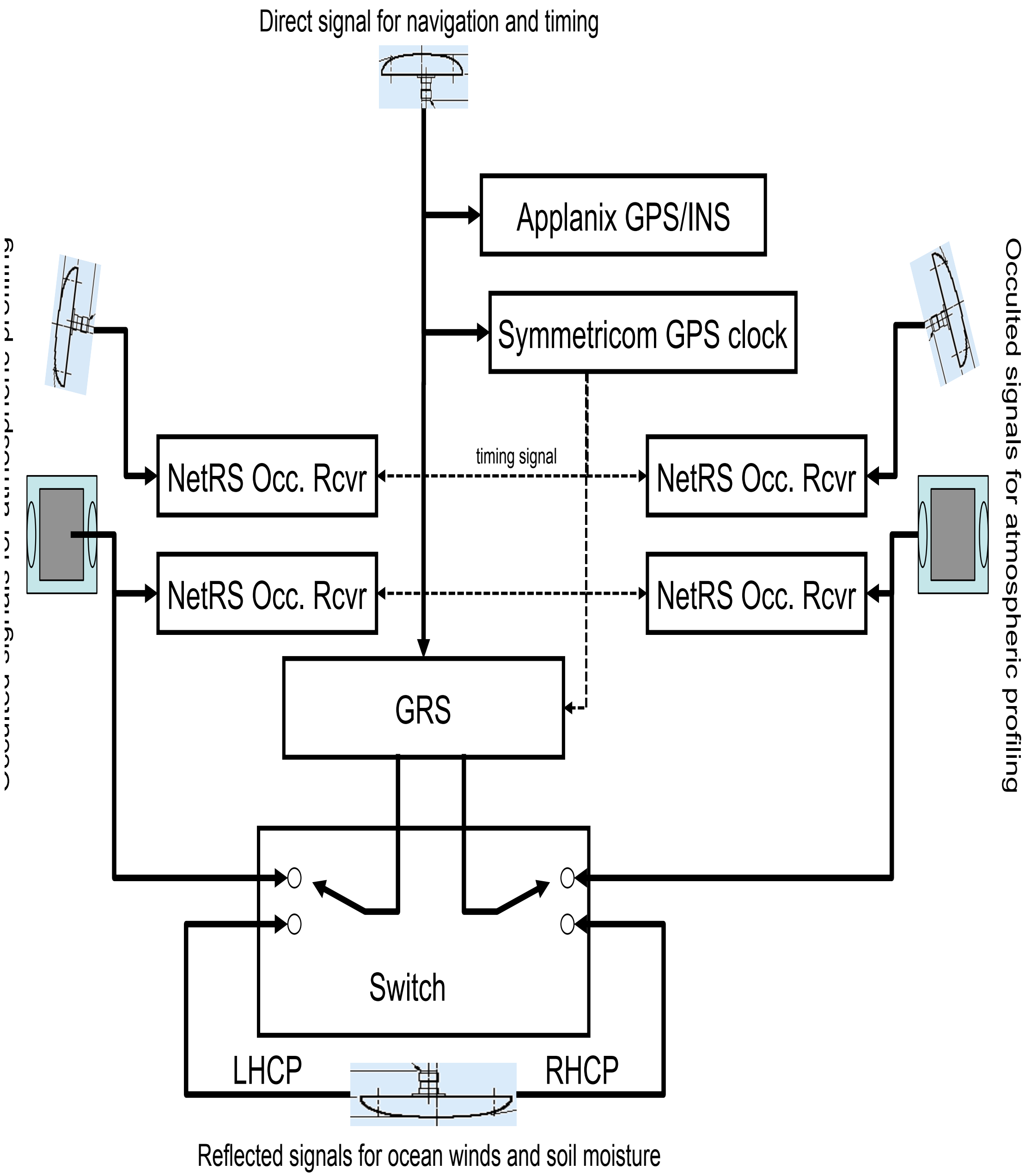

Direct signal for navigation and timing
Applanix GPS/INS
Symmetricom GPS clock
timing signal
NetRS Occ. Rcvr
NetRS Occ. Rcvr
NetRS Occ. Rcvr
NetRS Occ. Rcvr
Occulted signals for atmospheric profiling
GRS
Switch
LHCP
RHCP
Reflected signals for ocean winds and soil moisture

Ocean Reflection

- GPS reflection measurements can provide surface wind observations through heavy precipitation and clouds
- Down-looking GPS receiver records raw reflected signal from ocean
- Delay-doppler mapping of cross-correlation function gives surface roughness
- Surface wind speed is derived from the surface roughness

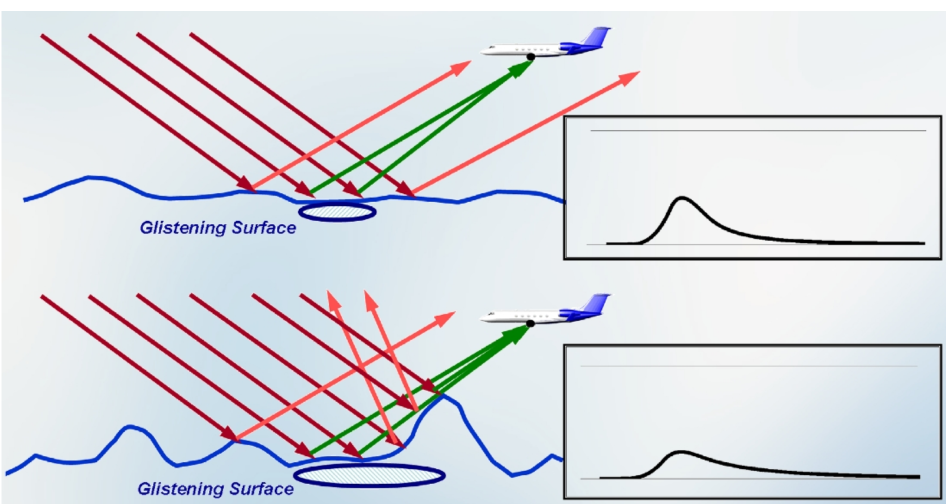

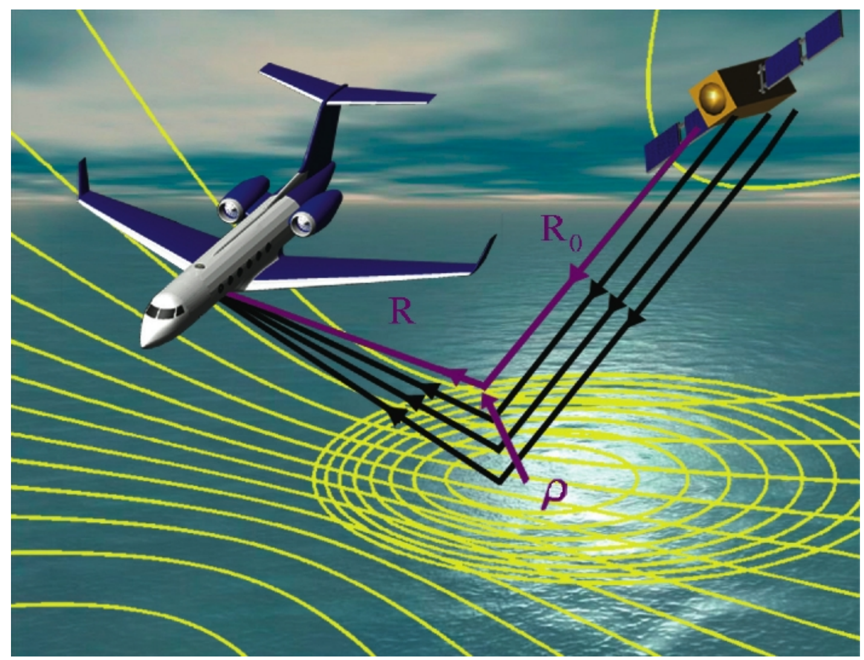

Land Reflection

- Down-looking GPS receiver records raw reflected signal from land surface
- Total power of scattered signal is related to the dielectric constant of the reflecting surface
- Soil moisture is derived from the dielectric constant

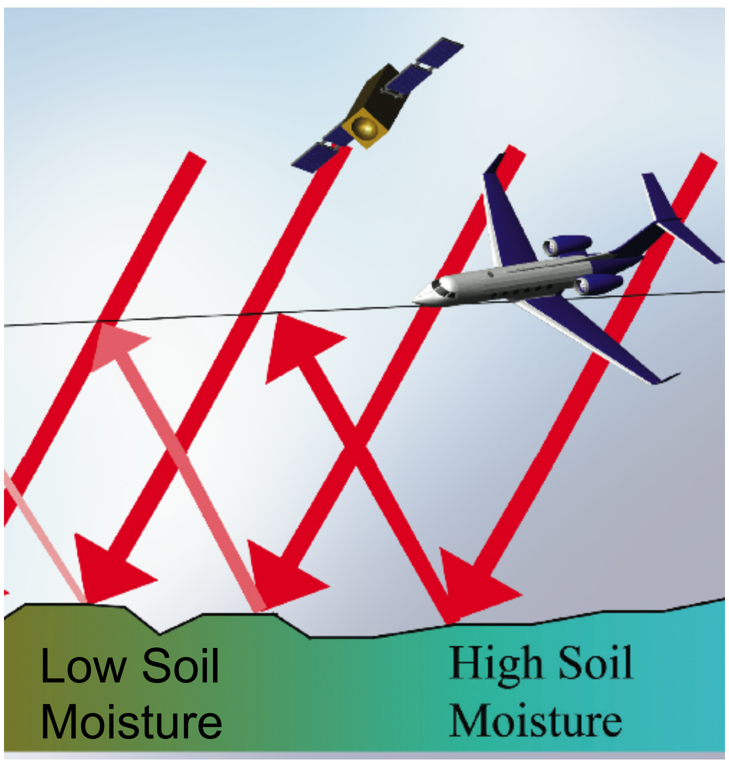

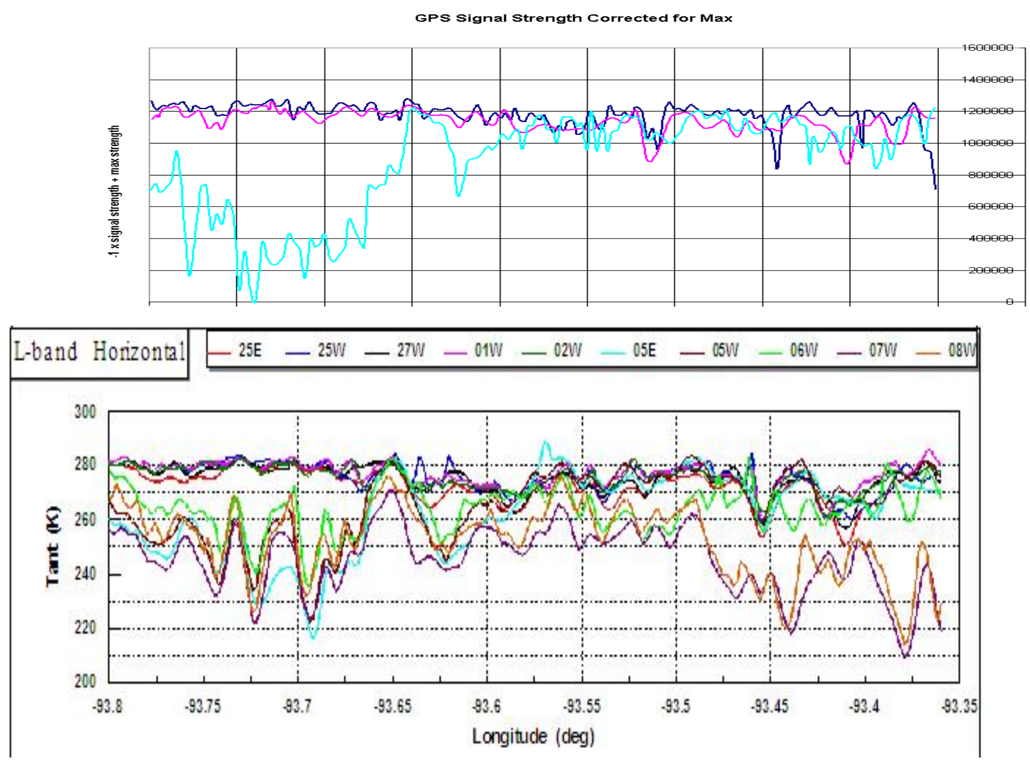

Focus on tropical waves

CIMSS MIMIC TPW product

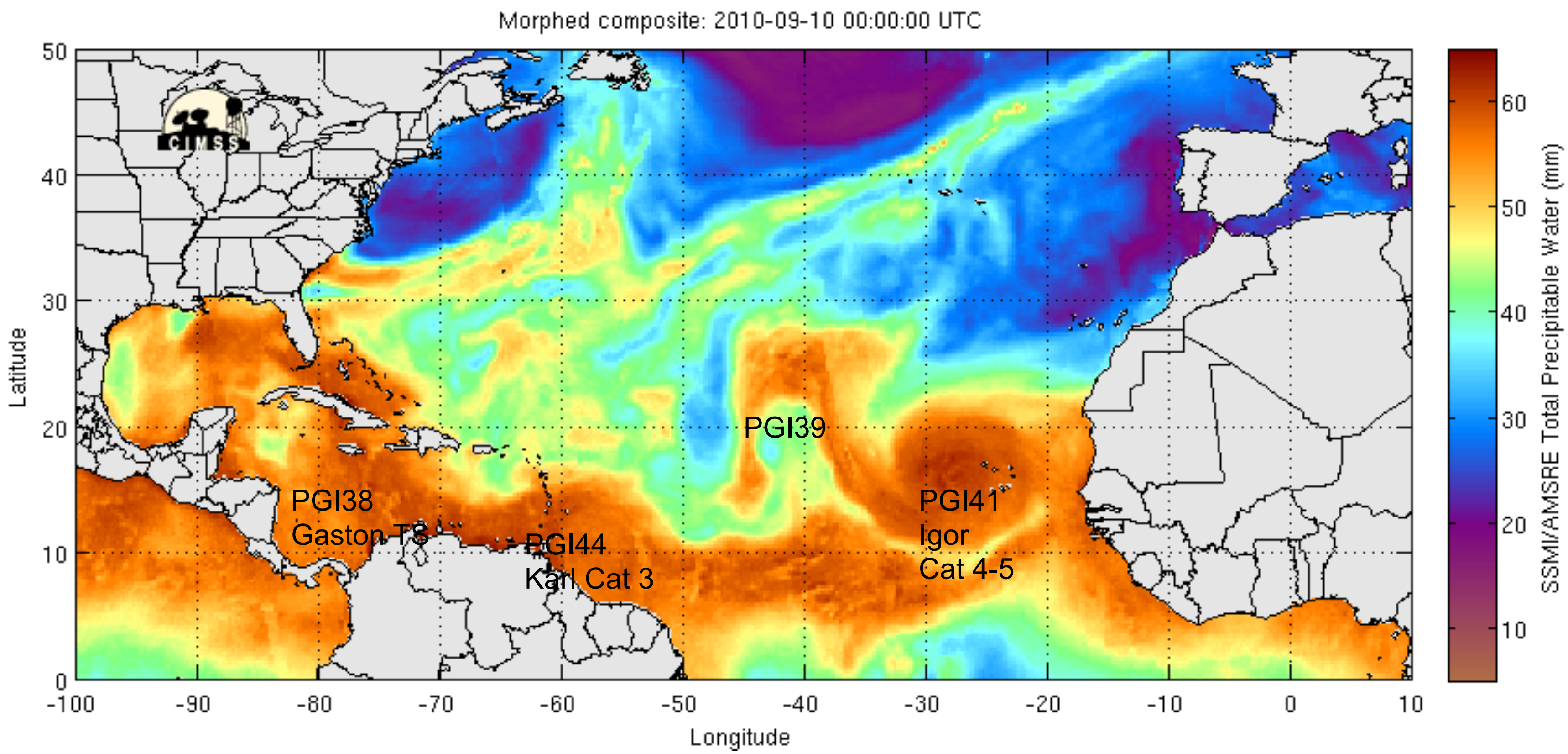

While more than 80% of intense hurricanes in the Atlantic originate as African easterly waves (Landsea, 1993) most easterly waves do not develop into hurricanes. Which waves will develop?

Development of Karl

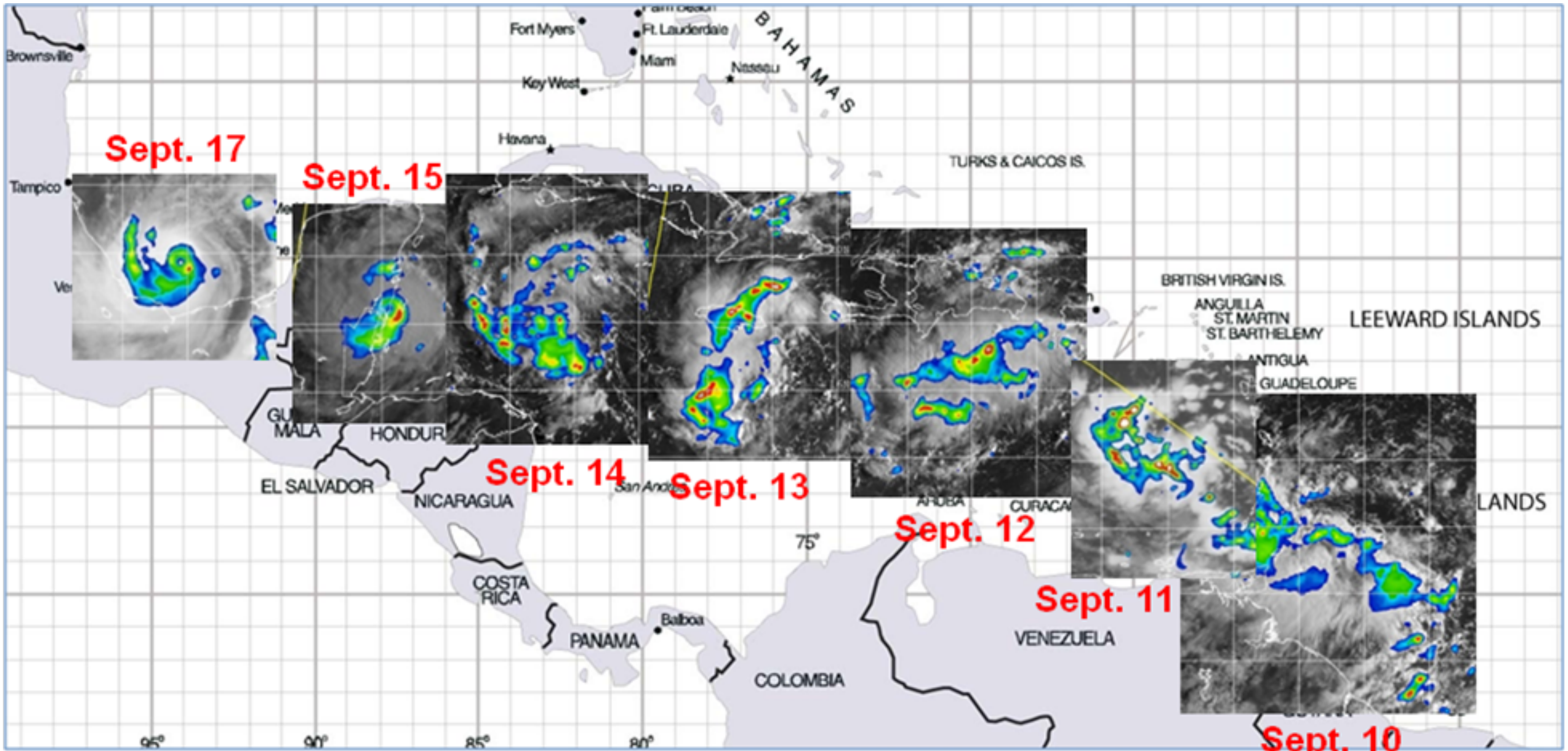

Hurricane ←Tropical Storm ←Depression ←------------------------Disturbance

Sept 16 18Z Sept 14 18Z Sept 14 12Z Sept 9

RF18 September 13, 2011

- PRN25 satellite occultation occurred near dropsonde 12
- NWP model reanalysis profiles are available on a 25 km grid

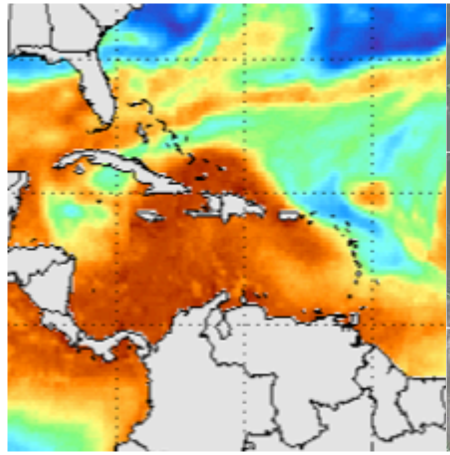

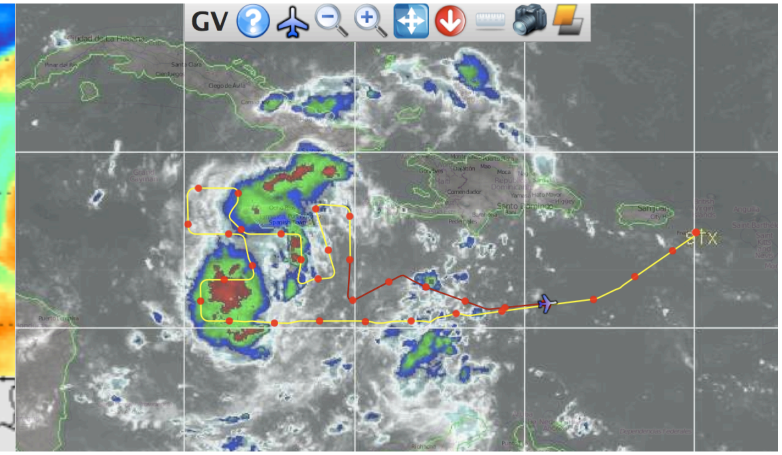

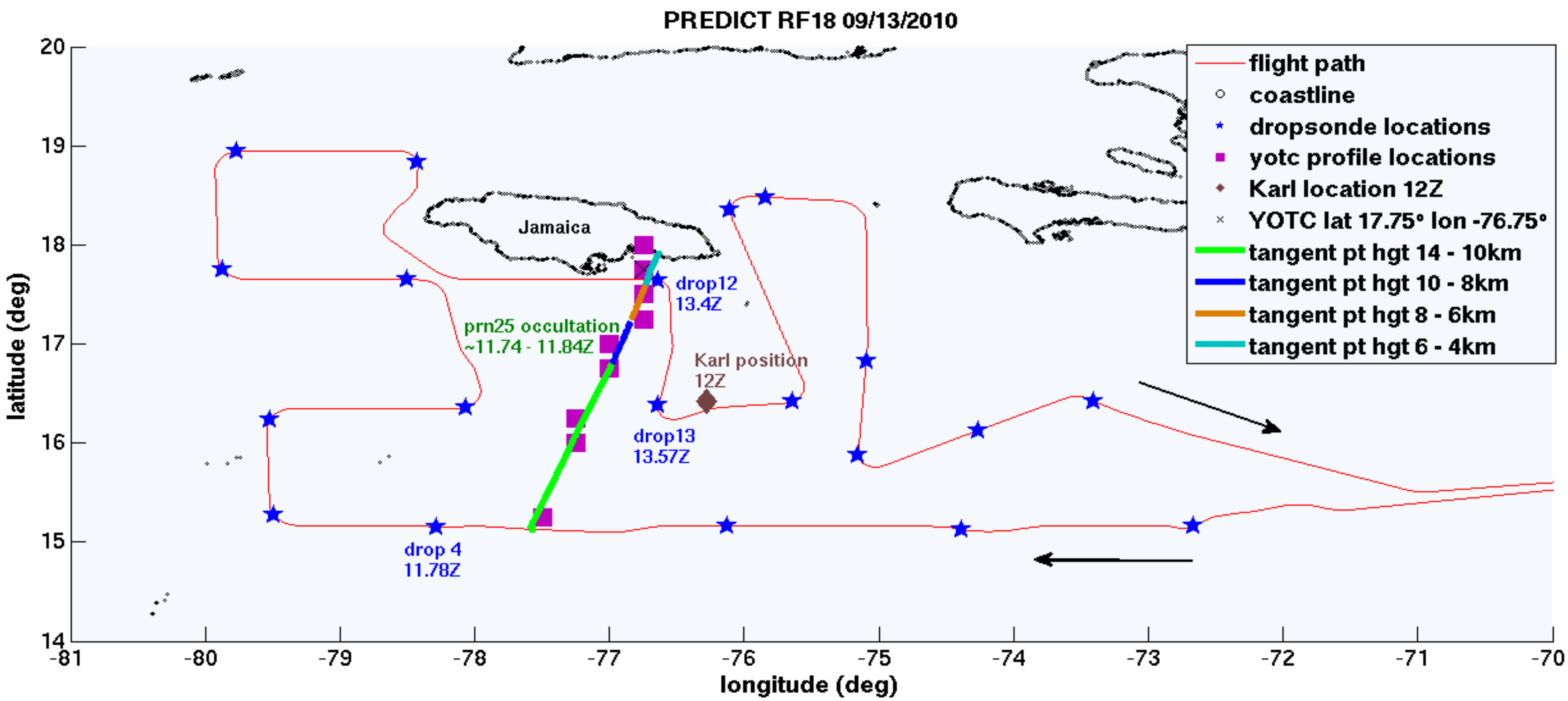

Comparison relative to the 4-day environmental mean

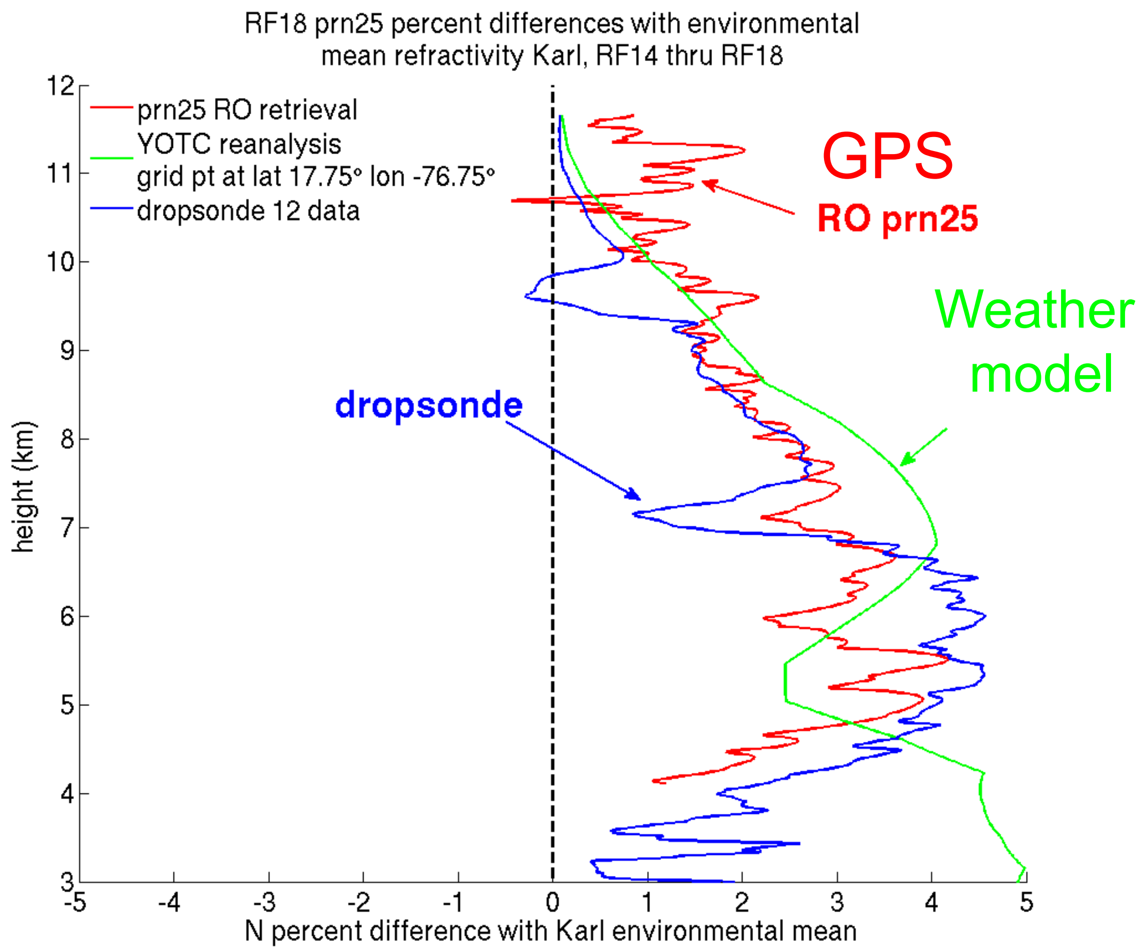

- GPS RO agrees well with dropsonde
- GPS RO differs from the current weather model
- All profiles are moister than 4-day mean

Flight Campaign

- Six research missions, RF14-RF18 sampled the pre-Karl environment from Sept 9 – Sept 14
- 14 to 16 dropsondes were released each flight
- Nine setting occultations were tracked by the GISMOS geodetic receivers

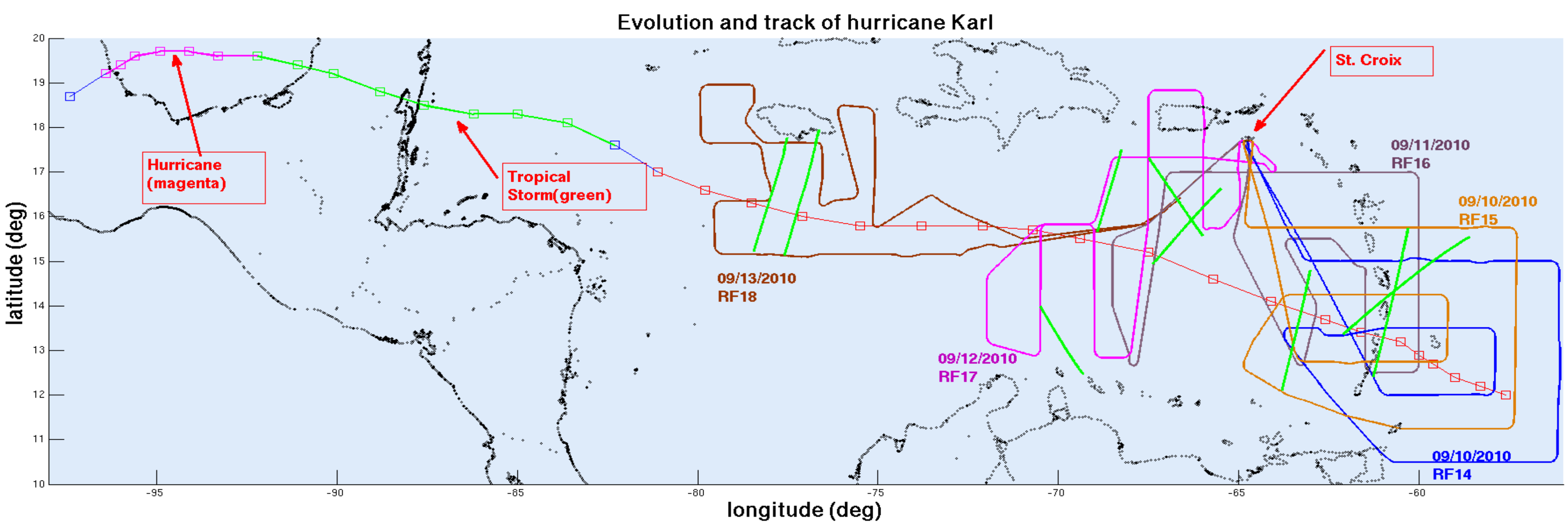

Pre-Karl moisture evolution

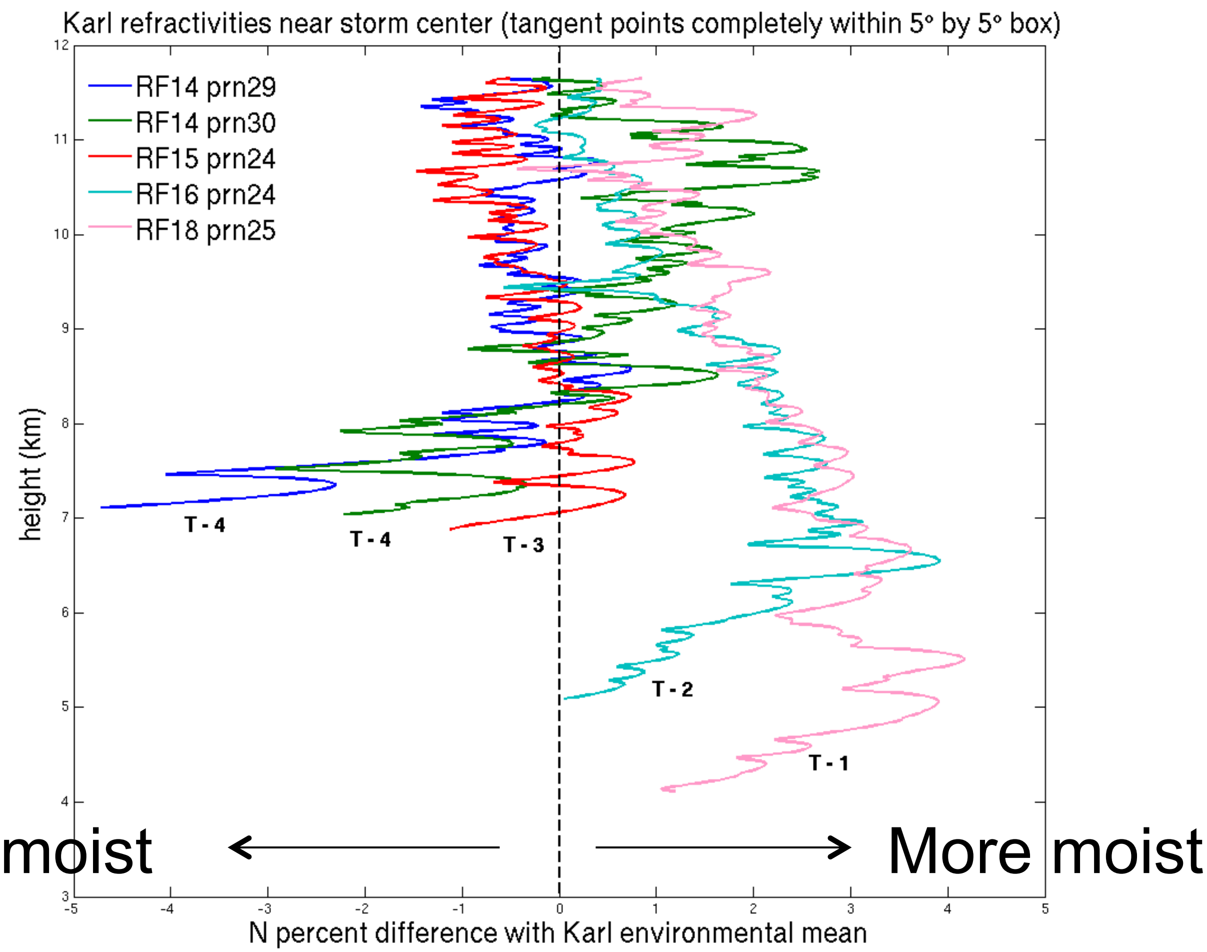

- The retrieved profiles are consistent with moisture increasing during the 4 day period before Karl reached the tropical depression stage.

Assimilation into the weather model

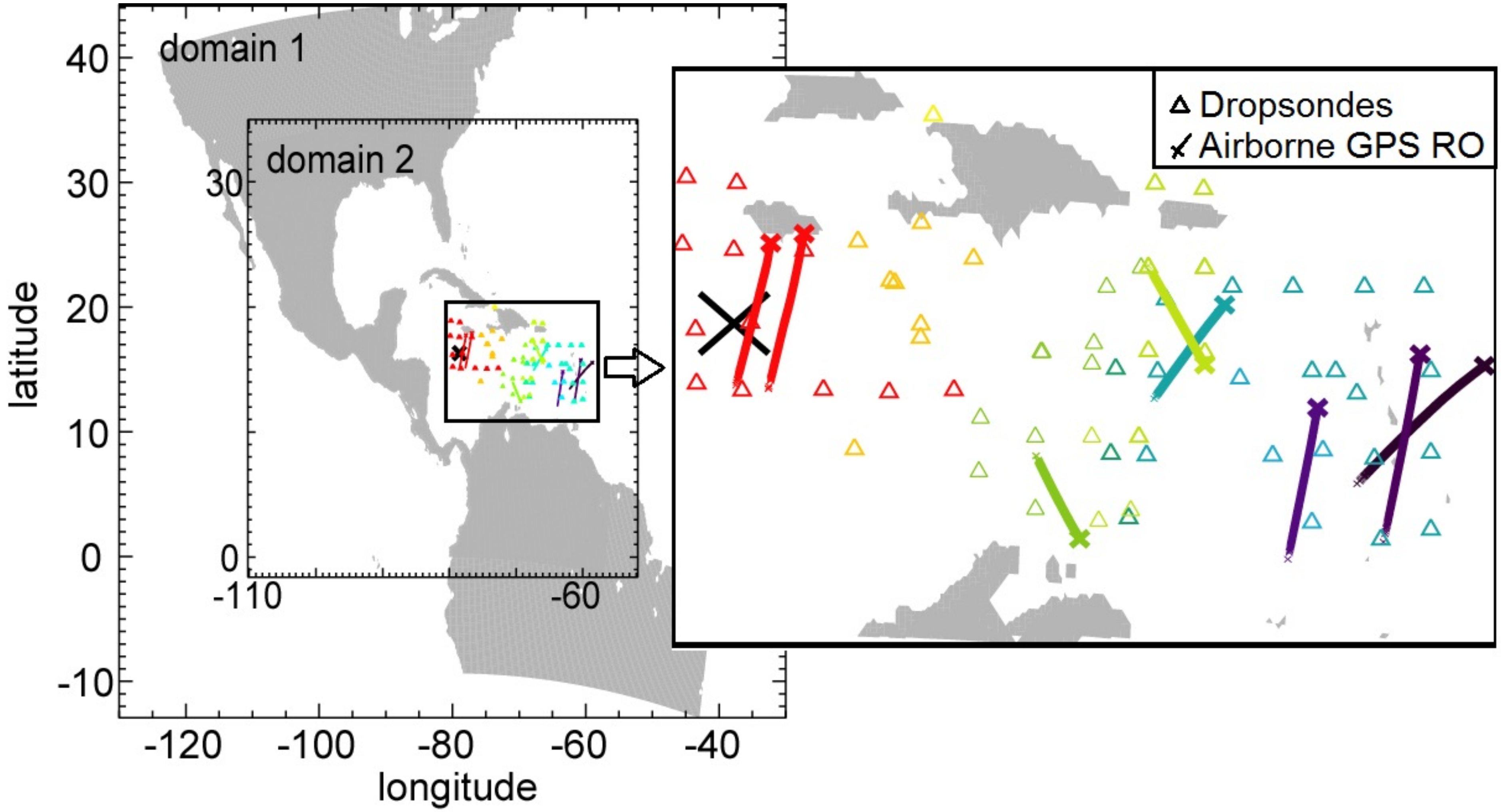

Weather model improvement

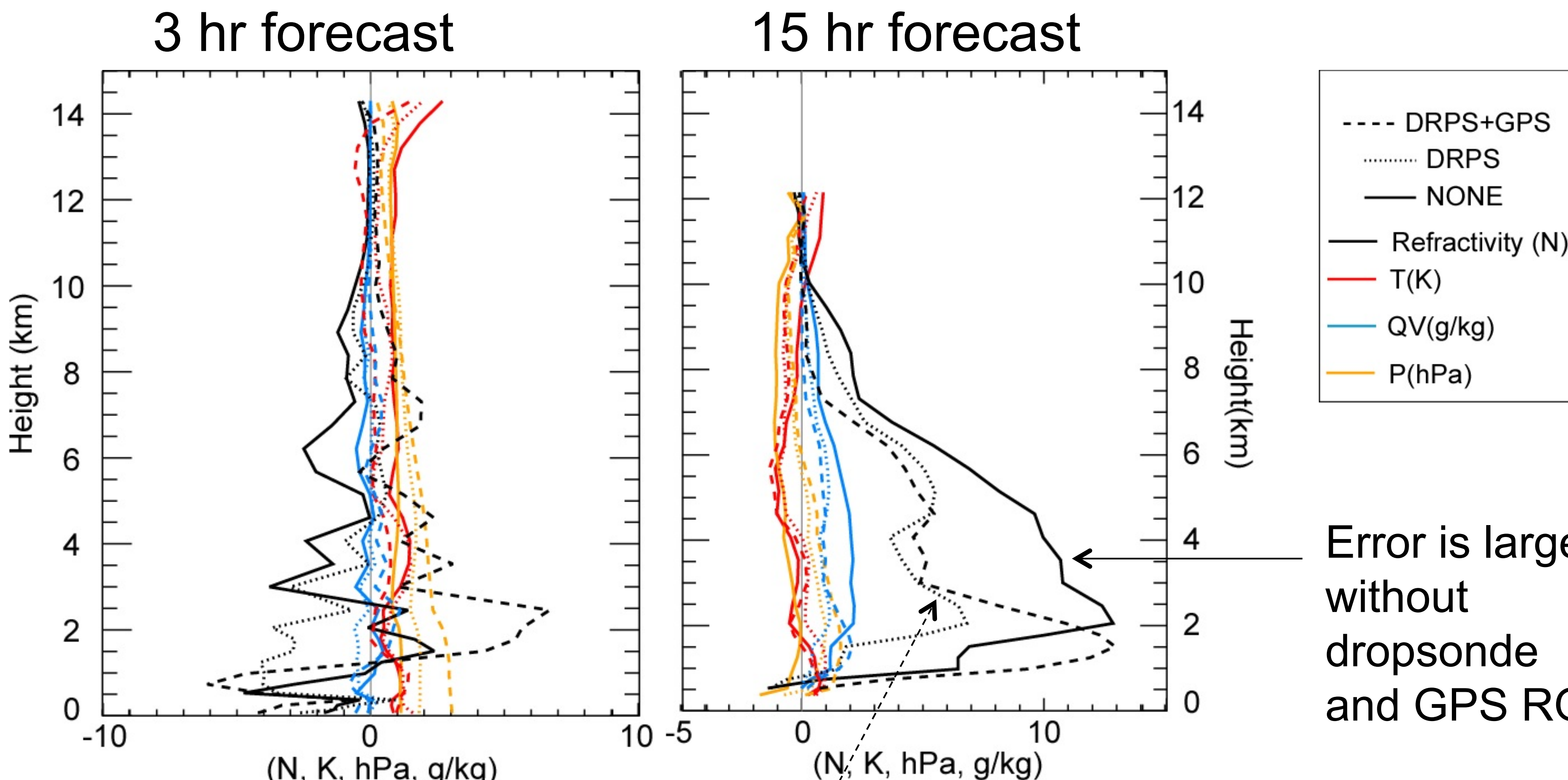

Error is larger without dropsonde and GPS RO

Error is smaller with dropsonde and GPS RO

Reasons for improvement

- PRN13 is located in a region of very high moisture
- PRN07 occurs in a very dry region.

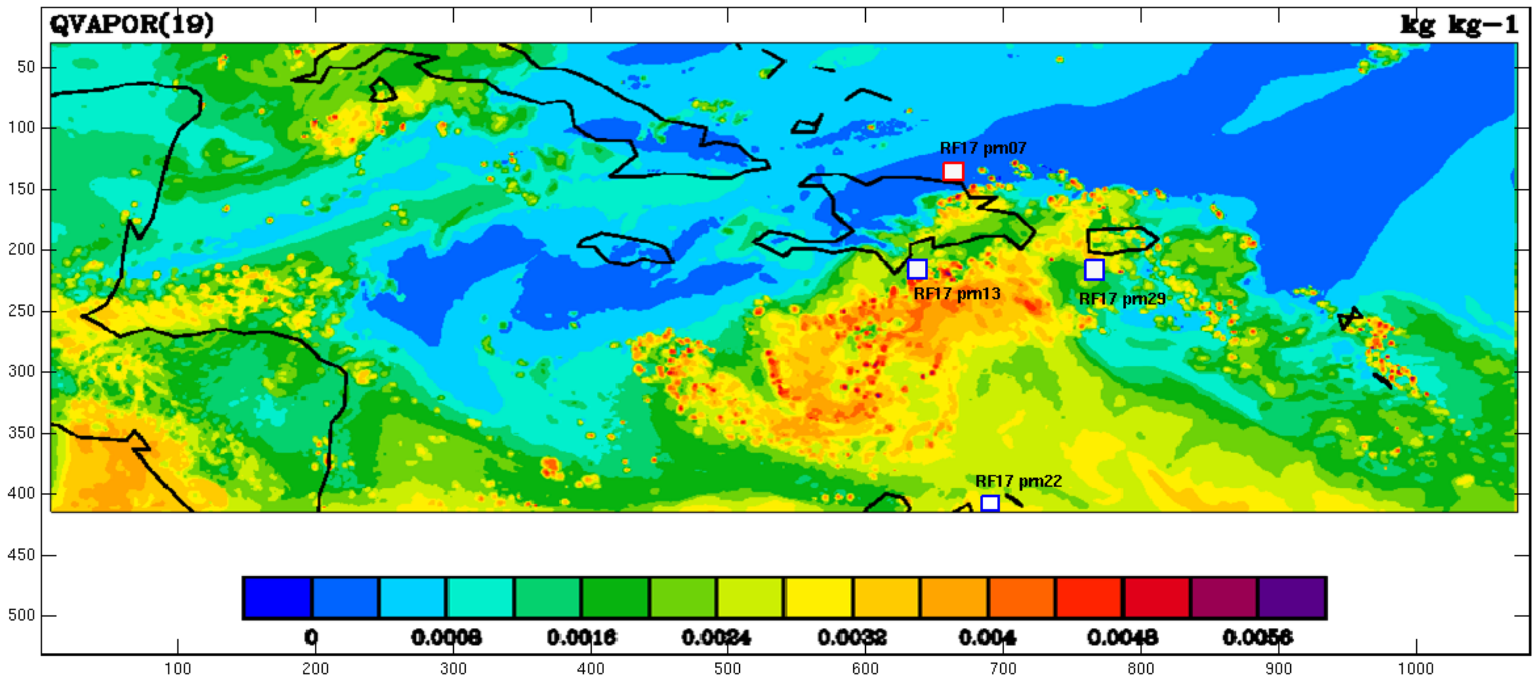

- New “open-loop” tracking technology will provide 7 times as many profiles so further improvement is expected

Summary and Future Work

- First comparisons demonstrate that RO profiles agree within 2% with refractivity of dropsonde profiles
- GPS RO refractivity profiles indicate increasing moisture over 4 days prior to development of hurricane Karl
- Assimilation of GPS RO and dropsonde data improved 15 hour weather model forecasts of moisture and refractivity from 2km to 10km, and temperature from 2 km to 5km
- New “open-loop” tracking technology will provide ~7 times as many profiles so further improvement is expected
- An extensive dataset from 28 flights and 8 tropical disturbances will provide more case studies of developing and non-developing systems

Observation geometry for pre-depression convective systems

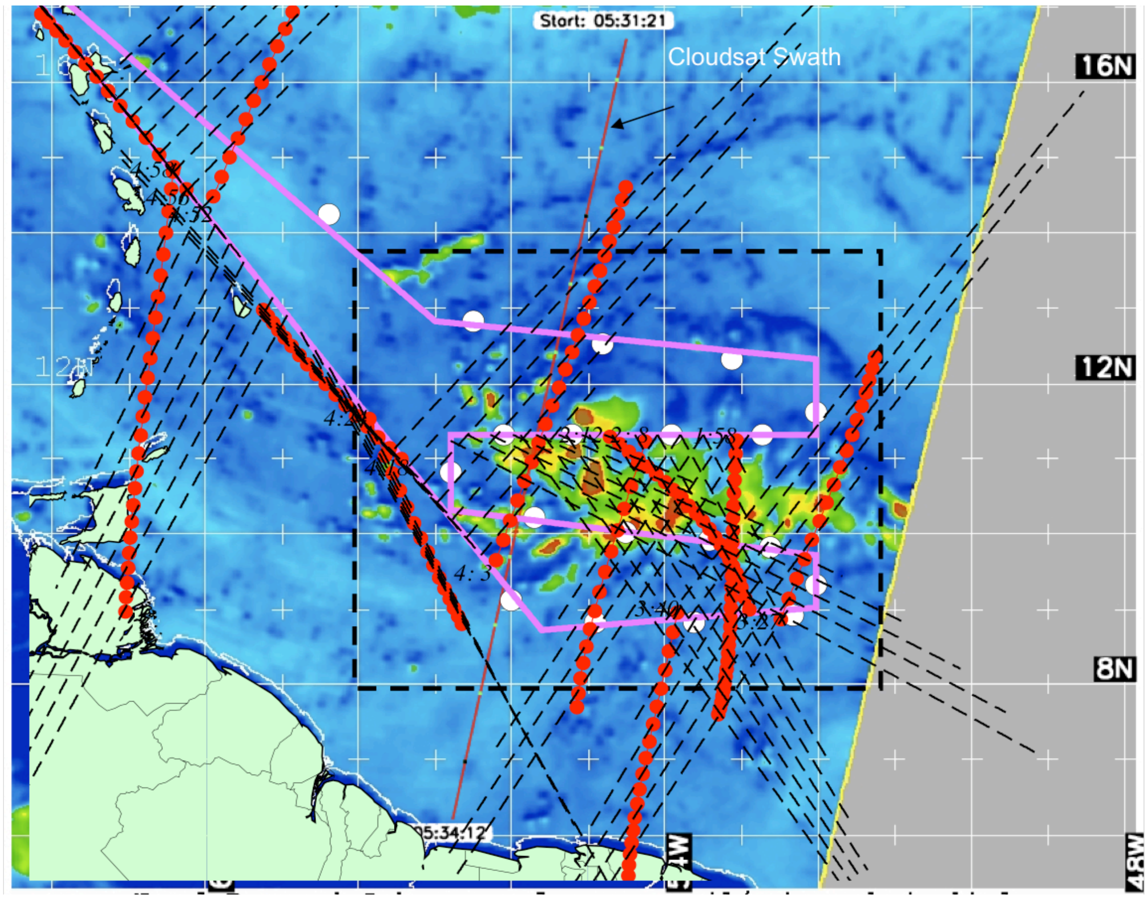

- High vertical resolution profiles can be retrieved through heavy precipitation.
- Targeted regions can be sampled with the aircraft far from potentially dangerous zones.
- Airborne RO can provide a sampling complementary to point measurements made by dropsondes.

GPS radio occultation theory

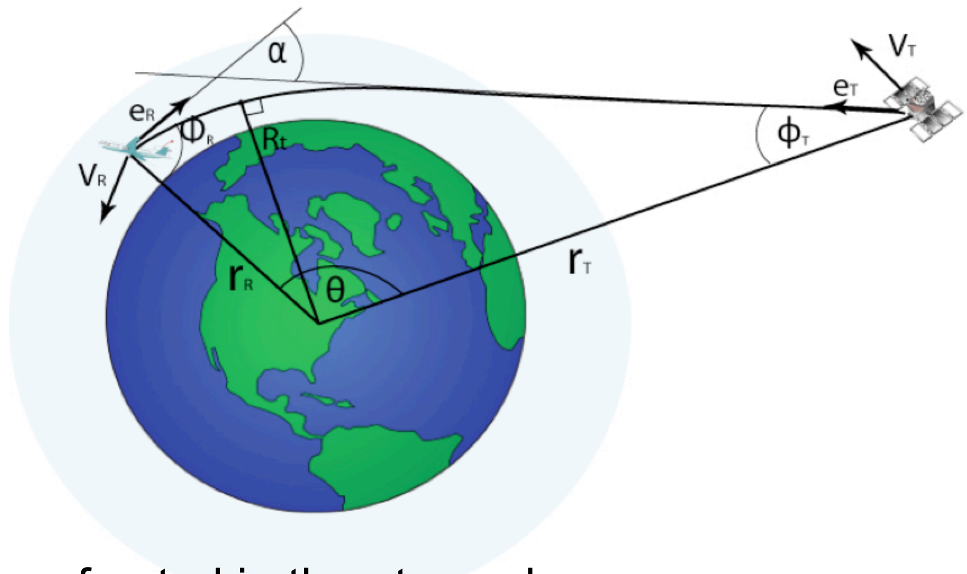

- GPS signals are refracted in the atmosphere
- Measure the difference between the observed distance and the straight line
- Refraction causes a Doppler shift in the carrier frequency
- The bending angle is an integral of the refractive index, which depends on P,T, and e

$$N = (n-1)\cdot 10^6 = k_1 \frac{P_d}{T} + k_2 \frac{e}{T} + k_3 \frac{e}{T^2}$$

Calculation of bending angle

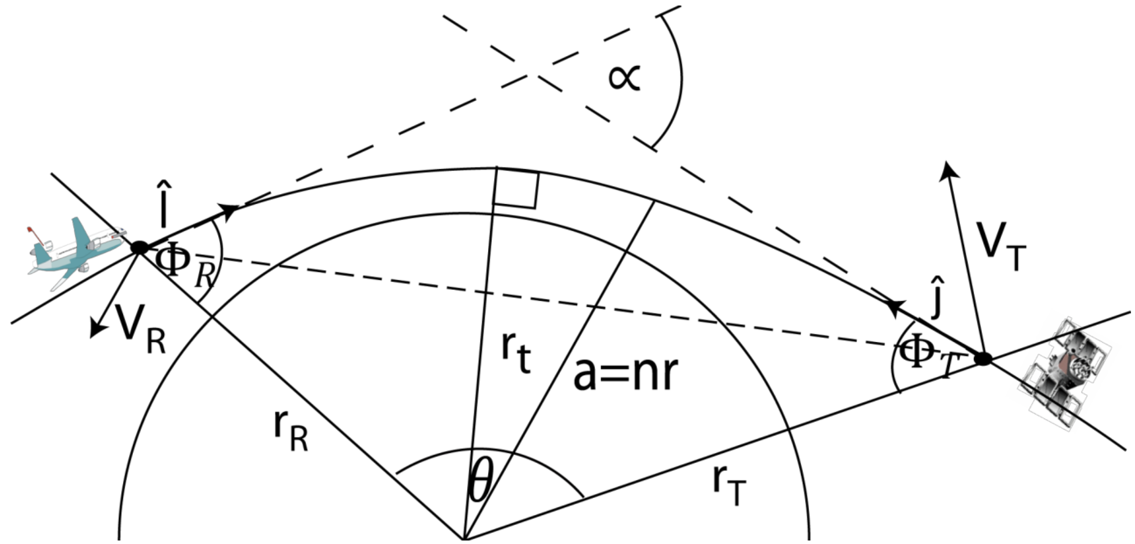

•From geometry: $\alpha = \phi_T + \phi_R + \theta - \pi$

•Snell's law: $n_R r_R \sin\phi_R = r_T \sin\phi_T = const = a$

•The bending can be derived from the Doppler shift

$$f_D = \frac{f_0}{c}(\vec{V}_T \cdot \hat{i} + \vec{V}_R \cdot \hat{j}) = -\frac{f_0}{c}(V_T^r \cos\phi_T + V_T^\theta \sin\phi_T + V_R^r \cos\phi_R - V_R^\theta \sin\phi_R)$$

Bending angle to refractivity

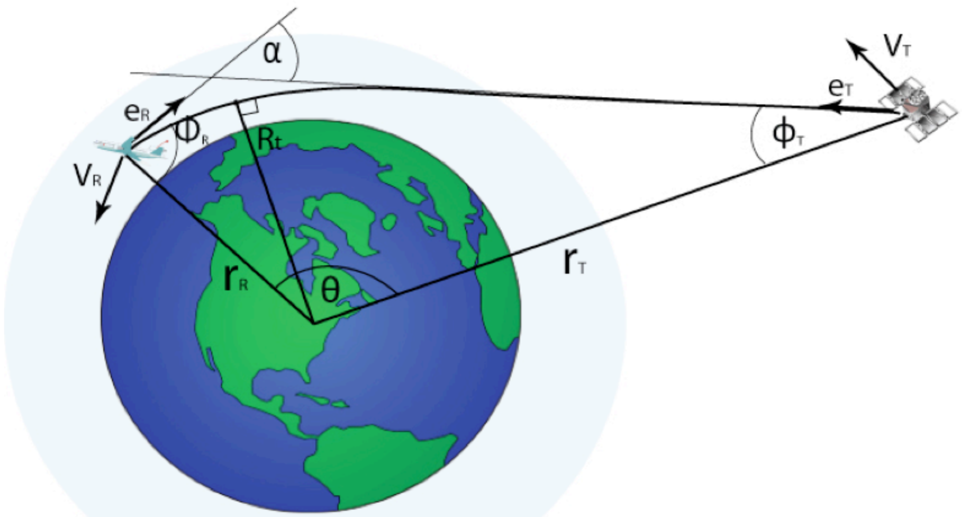

•The bending angle is an integral of the refractive index, which depends on P,T, and e

$$N = (n-1)\cdot 10^6 = k_1 \frac{P_d}{T} + k_2 \frac{e}{T} + k_3 \frac{e}{T^2}$$

$$\alpha'(a) = \alpha_N(a) - \alpha_P(a) = -2a \cdot \int_{r_t}^{r_R} \frac{1}{n}\frac{\mathrm{d}n}{\mathrm{d}r} \frac{\mathrm{d}r}{\sqrt{(nr)^2 - a^2}}$$

$$n(a) = n_{\mathrm{rec}} * \exp\left[\frac{1}{\pi}\int_a^{n_{\mathrm{rec}}R_{\mathrm{rec}}} \frac{\alpha_{\mathrm{partial}}(x)\,\mathrm{d}x}{\sqrt{x^2 - a^2}}\right] \text{, inverse abel transform}$$

Observable = phase data => Doppler shift=> Bending angle=> Refractivity=> T, humidity

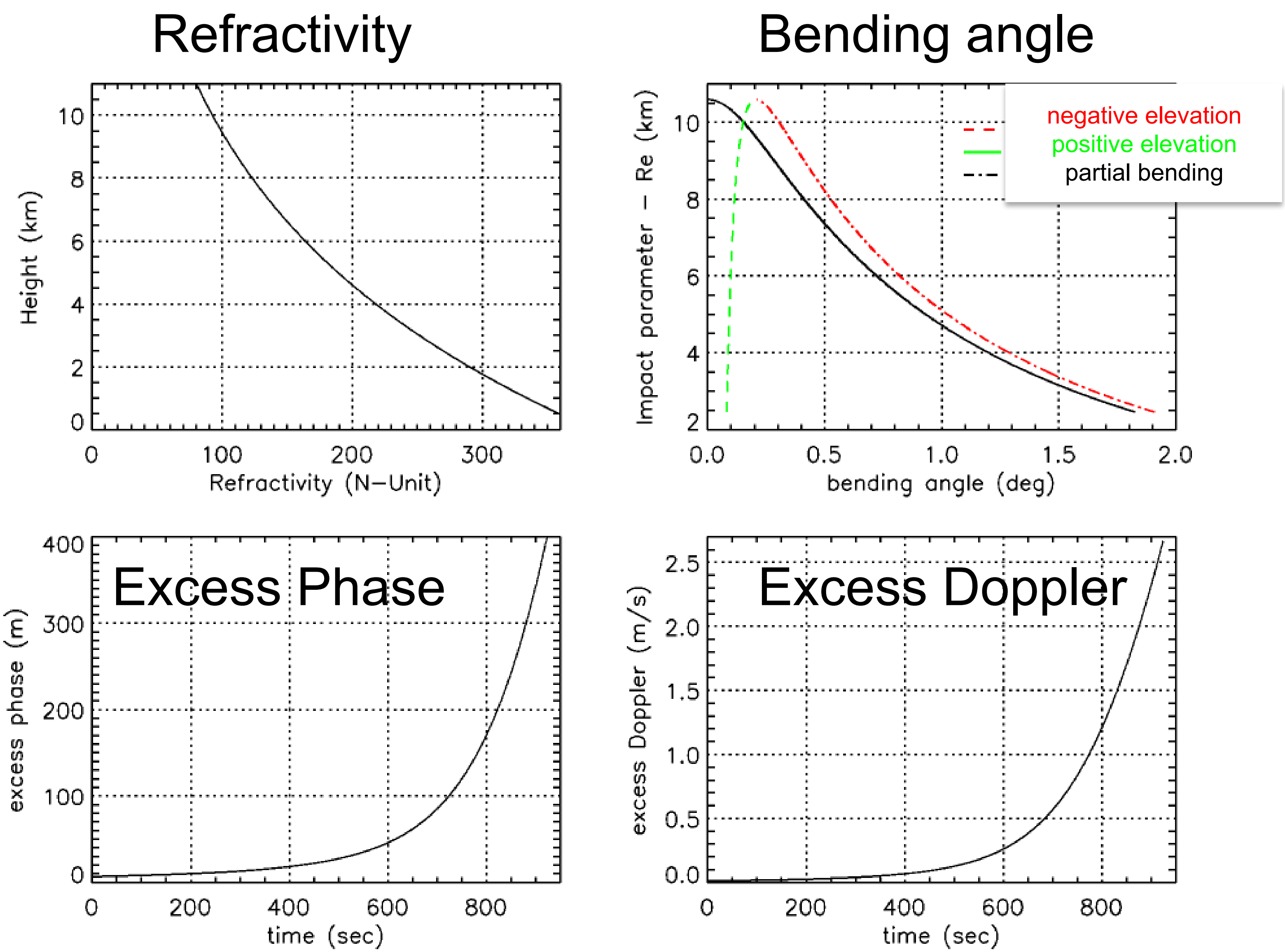

Challenging measurements: maximum doppler 2.5 m/s
velocity noise 0.005 m/s

• Excess Doppler is the derivative of the observed carrier phase minus the vacuum line-of-sight carrier phase

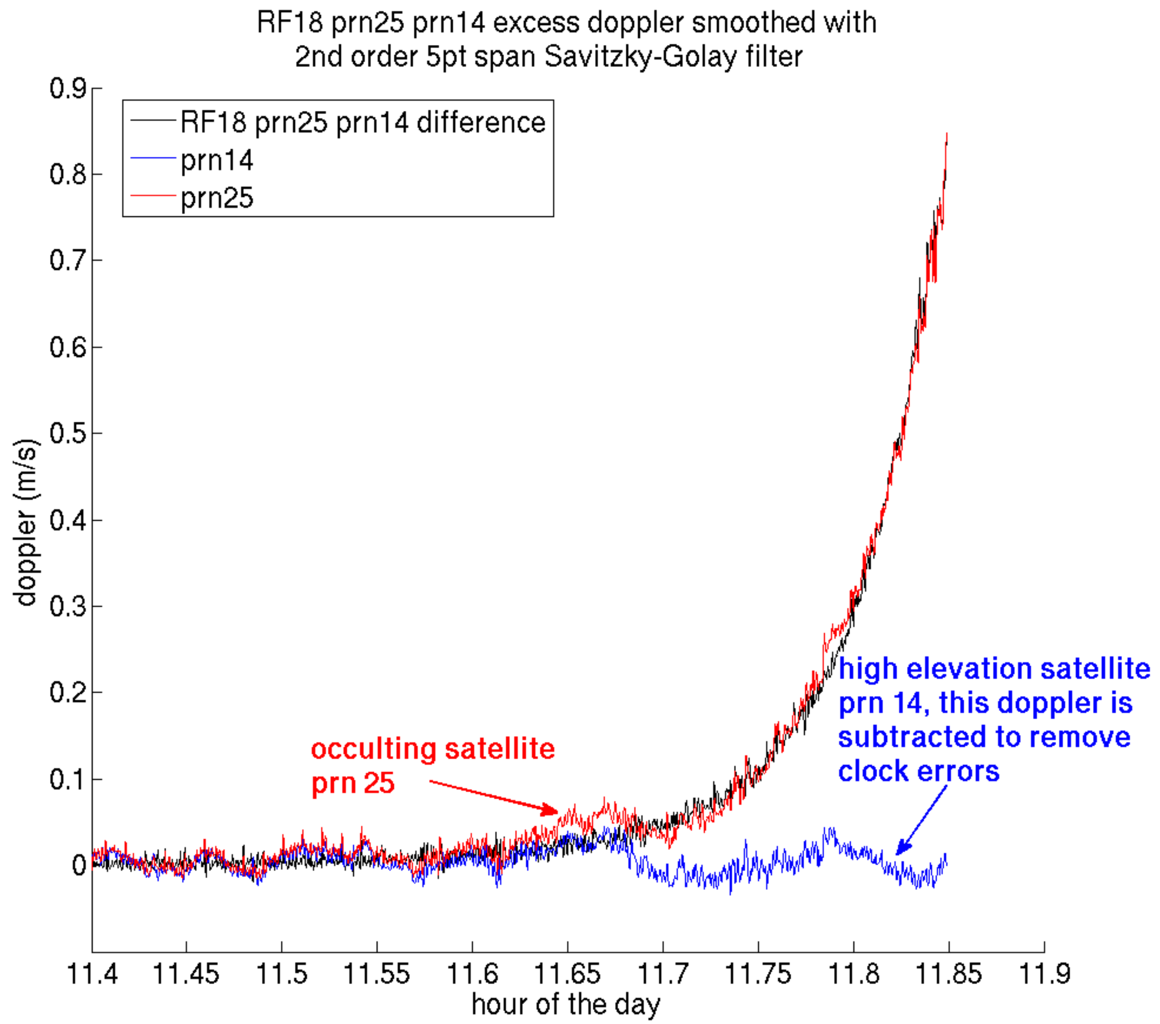

• Bending angle is calculated using geometric optics

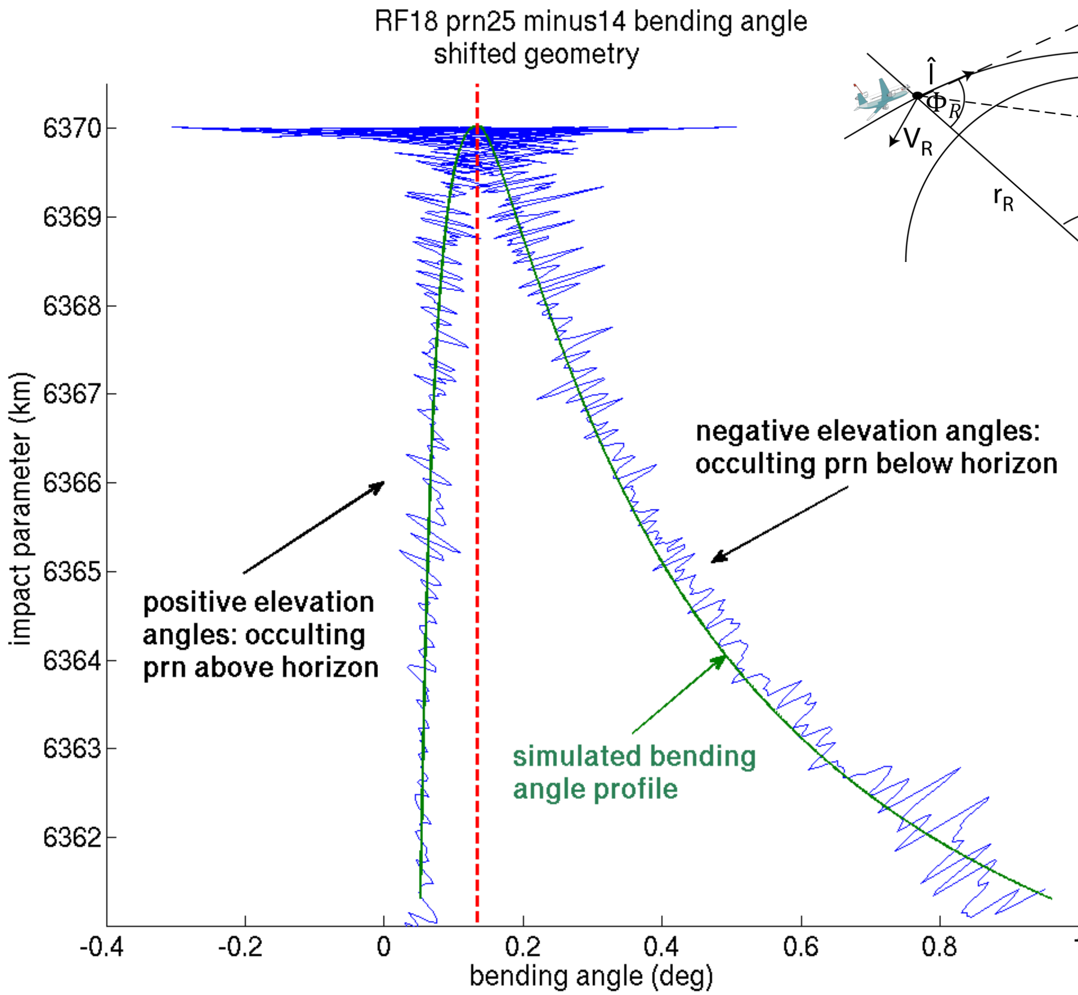

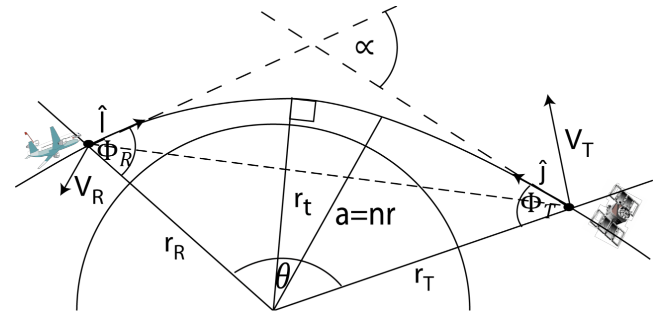

- Noisy section at top of profile is replaced with simulated bending angle
- Partial bending angle removes the effect of the atmosphere above the aircraft

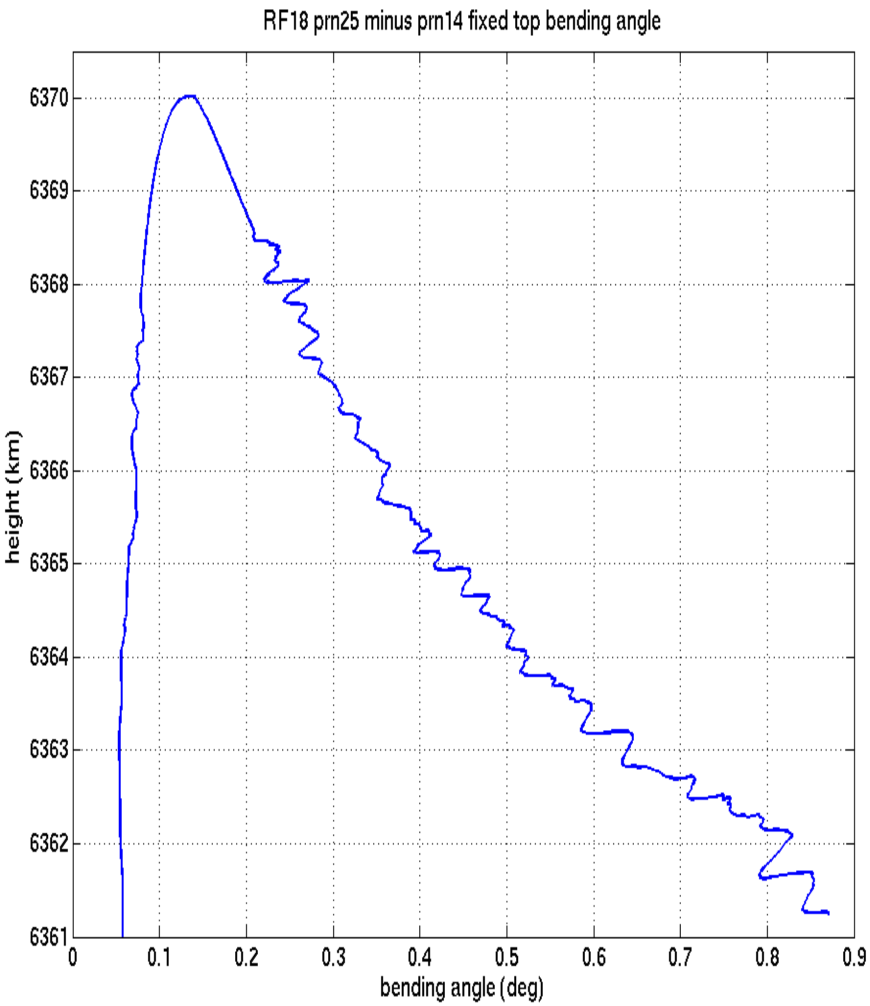

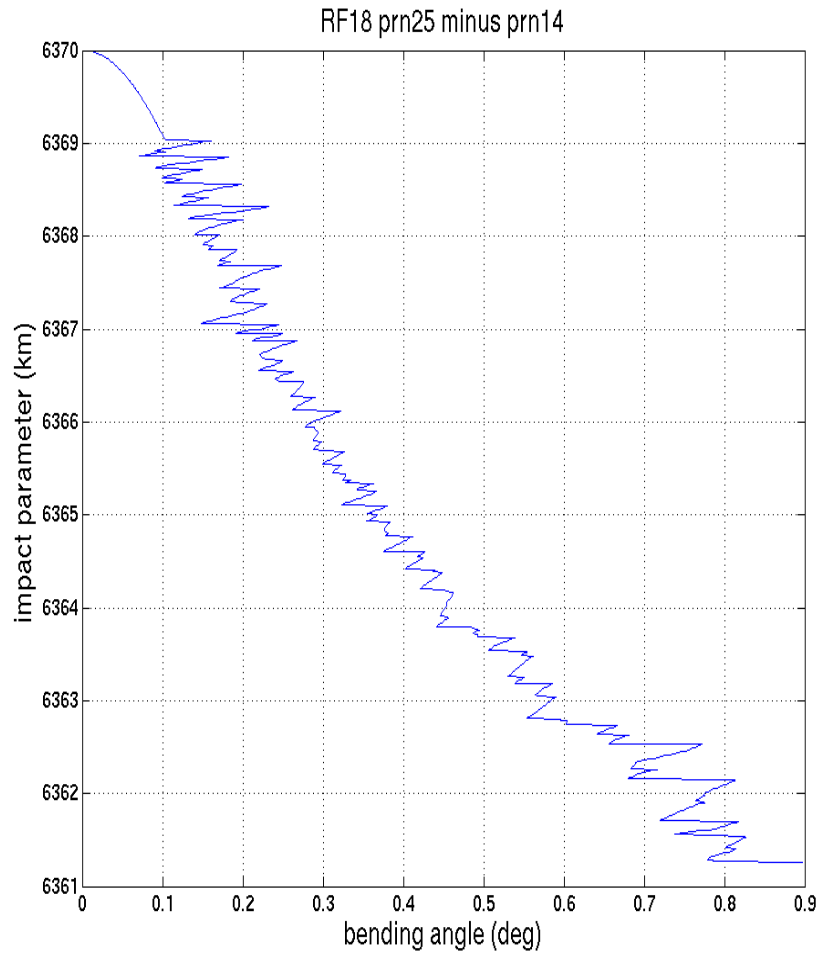

- Use inverse Abel transform to find refractivity

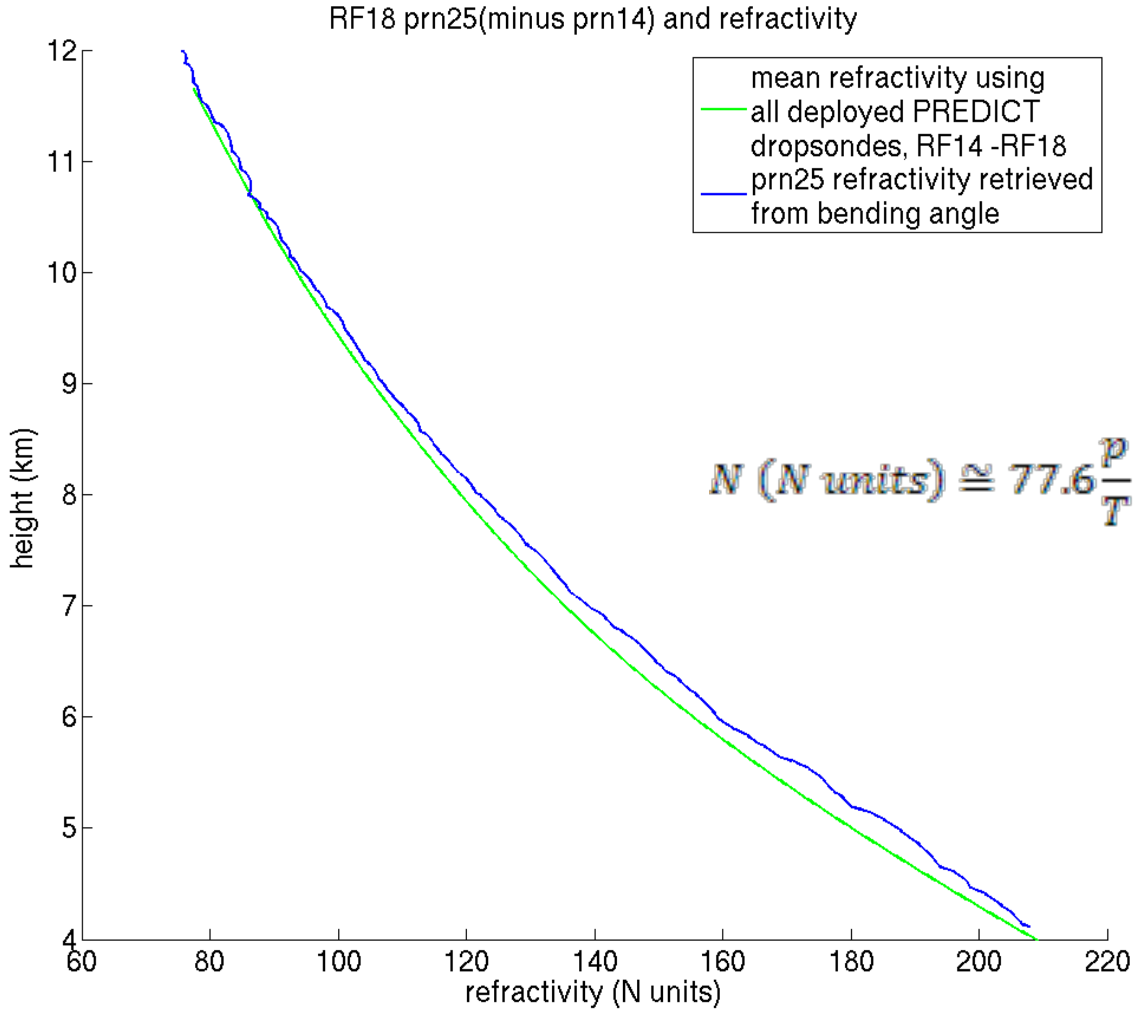

$$N\ (N\ units) \cong 77.6\frac{p}{T} + 3.73 \times 10^{5}\frac{e}{T^{2}}$$

- Sept 13 profile is more moist than 4 day environmental mean